THE COSMIC EXPLORER GRAVITATIONAL WAVE OBSERVATORY

Technical Note	**CE-T2300002-04**	2023/07/31

On the relative orientation of two Cosmic Explorers in the US

Salvatore Vitale[a], Duncan Brown, B. Sathyaprakash
[a] *MIT*

This is an internal working
note of the COSMIC EXPLORER project.

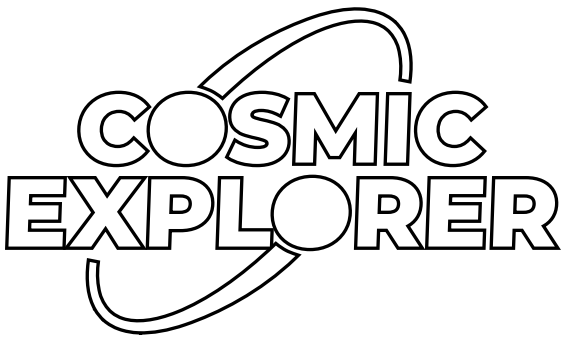

http://www.cosmicexplorer.org/

1 Introduction

In this note we analyze the impact of the relative orientation between two Cosmic Explorer (CE) sites in the US. We use the following two sites:

	Arm length	latitude	longitude	x-arm angle North of East
CE A	40 Km	46°	−125°	$200° + \delta$
CE B	20 km	29°	−94°	200°

Table 1: Position and orientation of the two CEs. The last column reports the angle that the x-arm of the detector makes North of the local East direction. In turn, the x-arm is defined as the one that completes a right-handed coordinate systems together with the other arm at the local outward vertical direction.

We notice that those two locations are unphysical, and do not correspond to corner stations on the continental landmass. This will not restrict the validity of our main conclusions, as the exact position of the detectors will not matter, within a few hundreds of kilometers.

In what follows, we keep the orientation of CE B relative to the local East fixed, and we vary the orientation of CE A. We parametrize the orientation of both detectors by specifying the angle that their x-arms make North of the local East directions, last column of Table 1.

For a network of today's detectors, there is no obvious "best" figure of merit to compare relative merits of different proposed networks [1, 2, 3]. For example, the two LIGO detectors have been built with arms that are roughly aligned, in order to maximize the probability of a first detection. That comes at the expense of accessing both GW polarizations, which would instead require detectors that are rotated by 45° (at least in the limit where the detectors were co-located, otherwise the curvature of the Earth must be accounted for).

We argue that the situation is very different for binary black holes (BBHs) in the XG era, and partially different for binary neutron stars (BNSs). The reason is that, barring major surprises in the high-redshift merger rate, CE does not suffer of a selection effect as severe as the one experienced by today's detectors [4] for BBHs, and suffers its by a smaller extent for BNSs.

2 Binary black holes

We simulate a population of binary black holes with masses and spins consistent with what LIGO and Virgo have measured in O3b. There is obviously no guarantee that this will hold true at high redshift, but it's a reasonable starting point. The redshifts are distributed according to the Madau-Dickinson star formation rate (SFR). Thus, we are (for now) neglecting the possibility of a significant high-redshift merger peak due to pop III or primordial black hole mergers. Everything (sky position, polarisation angle, etc) else is drawn randomly on the line or on the sphere.

We start by drawing samples for the astrophysical distribution and calculate their optimal SNRs *as measured by CE B*. We call "detected" signals with SNR>8 in CE B and stop the

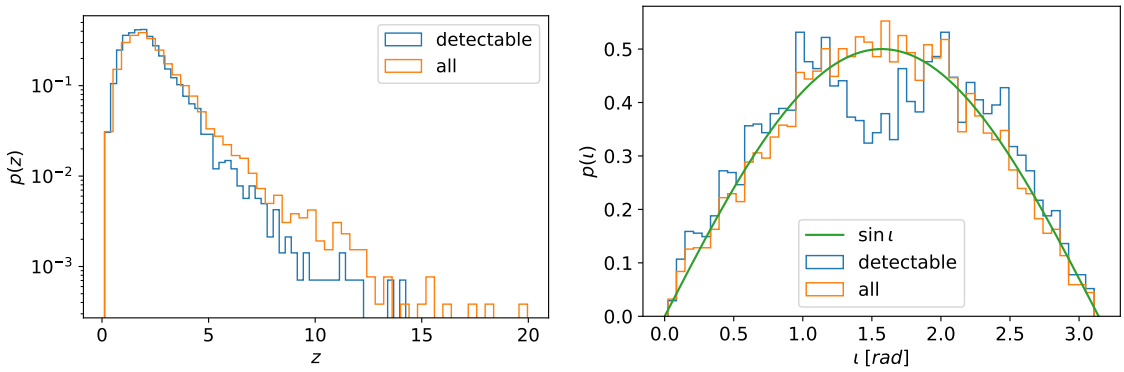

Figure 1: ((left) Distribution of redshifts for detectable (blue) and all (orange) binary black holes. The detection threshold is SNR 8 in CE B. (right) Distribution of inclination angles for detectable (blue) and all (orange) binary black holes. The solid green line represents the expected distribution for a fully isotropic distribution. The detection threshold is SNR 8 in CE B.

random sampling when we have acquired 5000 detectable sources. That happens when we have generated 6570 sources, i.e. 76.1% of the sources we generated are detectable. Most of the sources that are generated but missed, live at high redshifts, as shown in Fig. 1, left panel.

The right panel of Fig. 1 shows the distribution of inclination angles, and in particular how the distribution of detectable sources closely match the underlying $\sin\iota$ distribution, with only a small loss of events at $\pi/2$. We notice that this implies that for the majority of BBHs for which higher-order-modes can be neglected, the sensitivity to the plus polarization might be more important than that to the cross polarization, since this latter will be multiplied by a $\cos\iota$ term, which will be smaller for most sources [1]. This is very different from the typical source today, which will have inclination angle close to face-on, implying a comparable energy can be detected in the two polarizations.

It is not generally true that most sources for a CE 20 km detector will be overhead. That is shown in Fig. 2, which reports the sky position of all detectable sources. The location and orientation of CE B are also shown. The distribution of detectable sources is roughly uniform, with small "holes" visible along the direction of the detector arms. The color of the markers represent the sky- and polarization-dependent absolute value of the cross part of the antenna response.

Next, we consider all of the 6570 sources (some of which were below threshold in CE B) and calculate their SNRs in CE A for all values of δ from 0 to $\pi/2$.

Most of the sources will be above threshold in both detectors. Here we are interested on the number of sources that are below threshold even when considering the network SNR, and on whether that number changes significantly with the relative orientation of the detectors, δ.

[1] Again, this is not necessarily true when higher order modes are important, since those have different angular dependencies on the inclination angle.

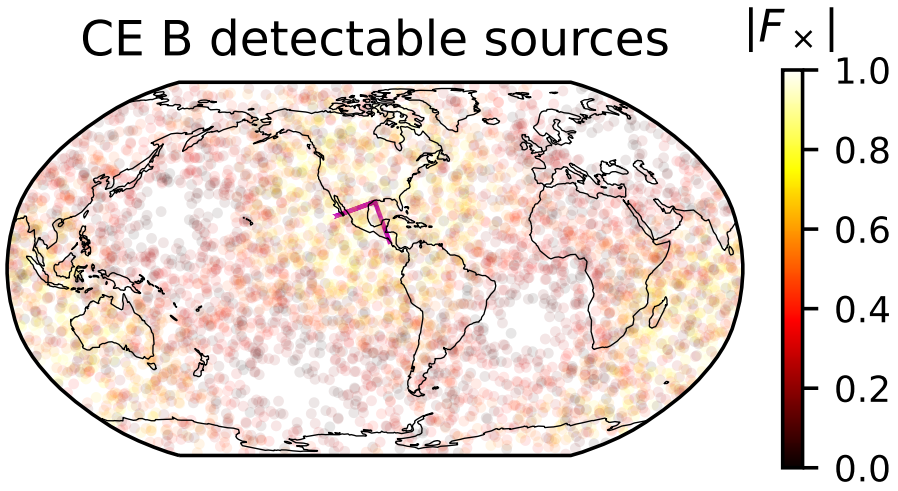

Figure 2: Distribution the sky position for detectable binary black holes. The detection threshold is SNR 8 in CE B. The color bar shows the absolute value of $F_\times$ in CE B. While gaps are visible, most sources are detectable irrespective of their sky position.

This is shown in Fig 3 where we show the fraction of undetectable sources (having *network* snr below 8 or 11) as a function of δ.

We see that that fraction is minimized for a relative orientation of around 60° and that there is a difference of $\sim 1.8\%$ [2] in the number of undetectable sources between the best and worst case scenario. For example, given 500,000 BBHs per year, the orientation would result in the number of detections to vary by $\sim 9,000$.

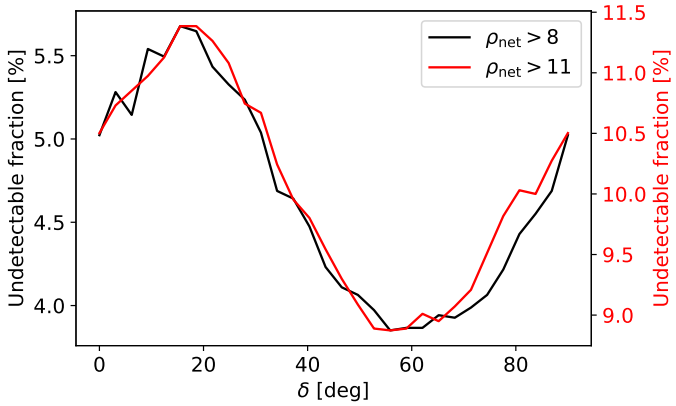

Figure 3: Fraction of sources that have network SNR below 8 (left axis) or 11 (right axis) in a network of CE A and CE B as a function of the relative misalignment between the detectors (see Table 1).

[2] Or $\sim 2.5\%$ when a network SNR threshold of 11 is used.

3 Sensitivity to the two GW polarizations

To gain some more intuition about the shape of the curve in Fig. 3 we try a different experiment. We pick a sky position just overhead CE B. Fixing (arbitrarily) the GPS time to 1126159642.413, that means ra= 6.1 and dec= 0.51, both in radians.

Then, we choose the value of the polarization angle ψ that *minimizes* the CE B response to the cross polarization. That turns out to be $\psi = 1.9$ rads.

With this sky position and polarization, the CE B reponse is

$$F_{+,\mathrm{CE\,B}} \simeq -1 \; ; \; F_{\times,\mathrm{CE\,B}} \simeq 0$$

We then ask the question of what δ should be such that CE A provides the largest response to the cross polarization, such that overall the network can probe both polarizations.

Fig. 4 shows how $|F_{\times,\mathrm{CE\,A}}|$ depends on δ. We see that it is largest at $\delta \simeq 68°$.

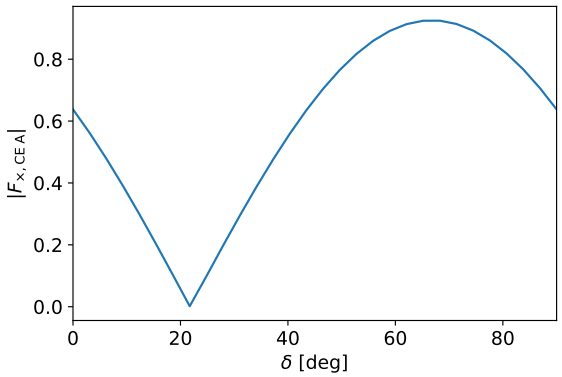

Figure 4: Absolute value of $F_\times$ for CE B for a source overhead CE A with $F_{\times,A} \simeq 0$.

One would obtain an identical result by fixing instead a ψ such that $|F_{+,\mathrm{CE\,B}}|$ is minimum for a source overhead CE B, and then look for the angle δ such that $|F_{+,\mathrm{CE\,A}}|$ is as large as possible.

This suggests that for BBHs the relative detectors orientation that yields the largest number of detections is the same for which the two detectors complement one another antenna patterns coverage. It is well know that for two co-located detectors, this would happen for two detectors with relative orientation of 45°. For detectors that are far away, one must take into account the curvature of the Earth. We do this in the next section.

4 Why 60 degrees?

The results above can be explained by realizing that given that CE B sees most of the BBH sources, there is no point on building CE A with a similar orientation: that would mostly serve at increasing the sensitivity in the regions where CE B antenna patterns are already

large. Instead, it is better to try increase the SNRs of marginal sources by accessing as much as possible of both GW polarizations. As mentioned above, if the two detectors were co-located, that would require $\delta = 45°$. Given the curvature of the Earth, we should instead expect something different. We can calculate the value of δ that maximizes the access to both polarizations by projecting the two arms of CE A in the plan of CE B's arms, as a function of δ.

In Fig. 5 we show in orange and green the smallest angle that either of the projections of the two CE A arms in the CE B plane form with the direction of CE B arms'. Intuitively, we want both of those to be as close as possible to 0.78 rads (i.e. 45°). Due to projection effects however, the two CE A arms in the CE B plane are *not* perpendicular to one another (blue curve). This is why the green and orange curve are not exactly overlapping. Therefore, in general we can't find a value of δ such that both the X and Y arms of CE A form an angle of 45° with CE B's arms once projected in CE B's detector plane. The next best thing we can do is to find a value of δ such that the sum of these two angles is as close as possible to 90° (A more complicated analysis would take into account the fact that the projection of CE A's arms do not have the same length. We will neglect this fact here since the lengths remain similar). The red curve in Fig. 5 shows the sum of the orange and green: that is our poor man's figure of merit for both arms of CE A being misaligned relative to CE B. We see that it peaks between 1.1 and 1.2 rads, that is between $\sim 62°$ and 68°, similarly to what we found numerically.

Finally, if Fig. 6 we show the arms of CE B (black) its local frame, and the projected arms of CE A (blue) when $\delta = 60°$. We see that, indeed, this is a relative orientation for which the arms of CE A and CE B, once projection effects are accounted for, are highly complementary.

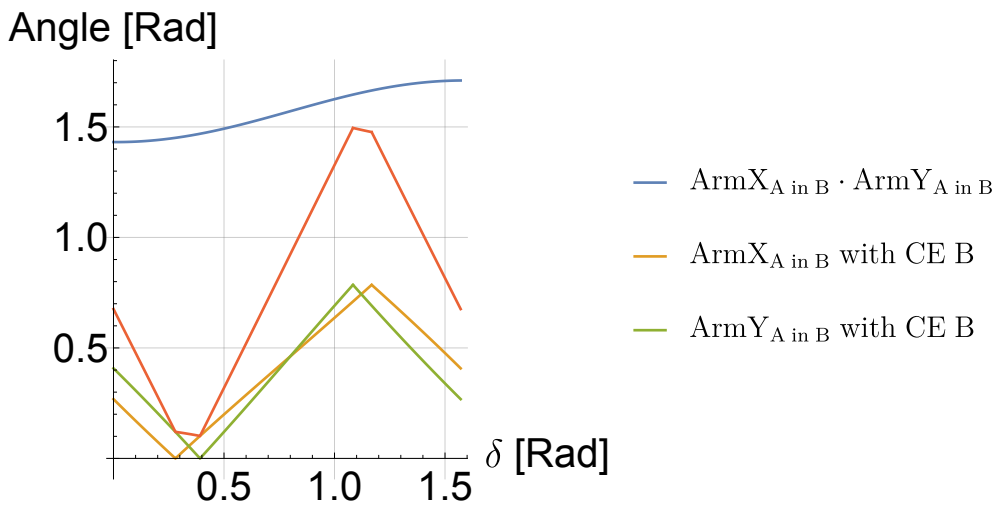

Figure 5: Blue curve: the angle between the projections of the two CE B arms in the CE A plane. Orange and blue curves: the smaller angle that the projections of CE B's X and Y arms make with either of the CE A arms. For δ between 1.1 and 1.2 – i.e. between $\sim 62°$ and 68° – the angle is $\sim 45°$. Red curve: the sum of the orange and green curves.

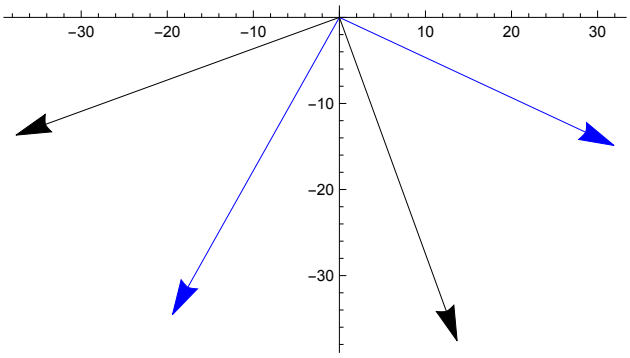

Figure 6: The arms of CE A (blue) projected in the plane of the CE B's arms (black), when $\delta = 60°$.

5 Binary neutron stars

We now repeat our population analysis for BNSs. We simulate a population of BNS with both component masses drawn from a truncated normal with $\mu = 1.4M_\odot$, $\sigma = 0.2M_\odot$, $m_{\rm min} = 1M_\odot$ and $m_{max} = 2.6M_\odot$. We set spins to zero, and again draw redshifts from the Madau-Dickinson SFR. We generate injections till we collect 5000 sources with SNR$>$ 8 in CE B. That requires simulating $\sim 73,400$ sources, i.e. only 6.8% of them are detectable by the 20 Km CE B alone.

Unlike for BBHs, we see a significant depletion in the distribution of detectable inclination angles, left panel of Fig. 7: selection effects for BNSs are just as severe as for advanced detectors (compare blue histogram and green curve, from Ref. [1]). The right panel of Fig. 7 shows that most sources at redshift above a few are missed. However, given the large uncertainty on the merger rate of BNSs at these redshifts, our numbers should be taken with a grams of salt: the actual detection efficiency of a single 20 Km might be higher than what we calculate here. The sky positions of BNS detectable by a 20 Km CE B clusters above and below the detector, Fig. 8, just as for current detectors. The fact that selection effects for BNSs with a single 20 Km CE are much more severe than form BBHs suggests that we should *not* expect that the relative orientation that maximizes polarization coverage will also maximize the number of BNS detections. Quite the contrary, we should expect to find a tension between polarization coverage and number of detections, just as for today's detectors.

To verify this, we repeat the same exercise we have performed for BBHs, and ask what fraction of BNSs are undetectable once we add CE A to CE B, with different values of δ, Fig. 9. We see that in this case, indeed, when $\delta \sim 60$ the number of undetectable sources is now *highest*: when selection effects are important, detections are maximized by aligned arms (which, modulo projection effects, would correspond to $\delta \sim 20°$). However, the number of undetectable sources only varies by less than 0.5% as δ is varied, making its choice even less consequential than for BBHs.

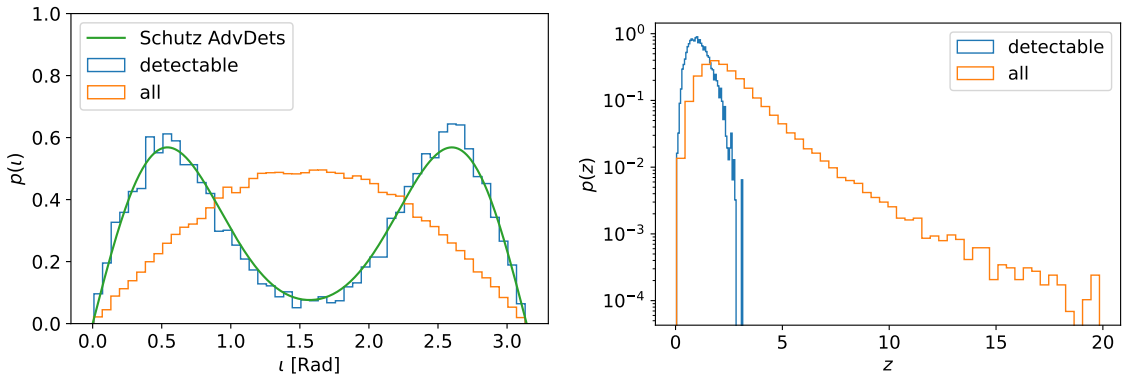

Figure 7: (left) Blue histogram: distribution of inclination angles for BNSs detectable by CE B. Orange histogram: distribution of inclination angles for all BNSs. Green curve: distribution of inclination angles for sources detectable by advanced detectors, from [1]. (right) distribution of the redshift for detectable (blue) and all (orange) BNSs.

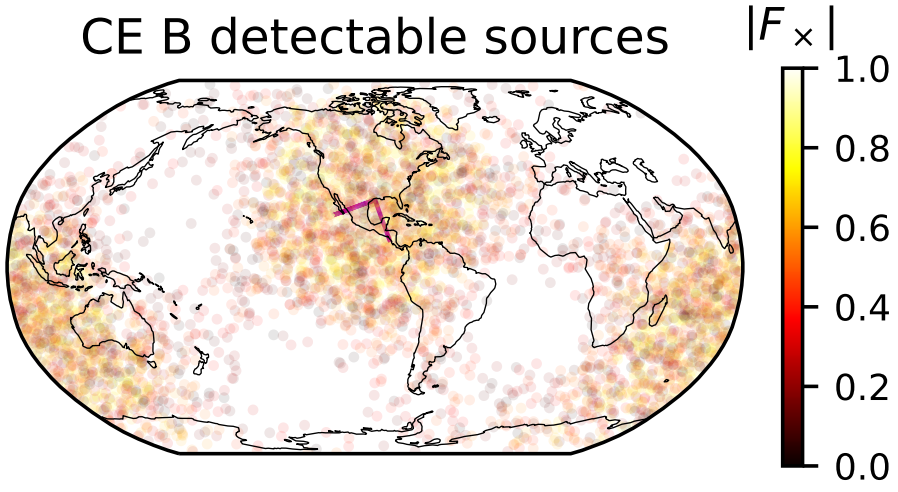

Figure 8: Distribution the sky position for BNS detectable by CE B. The color bar shows the absolute value of $F_\times$ in CE B.

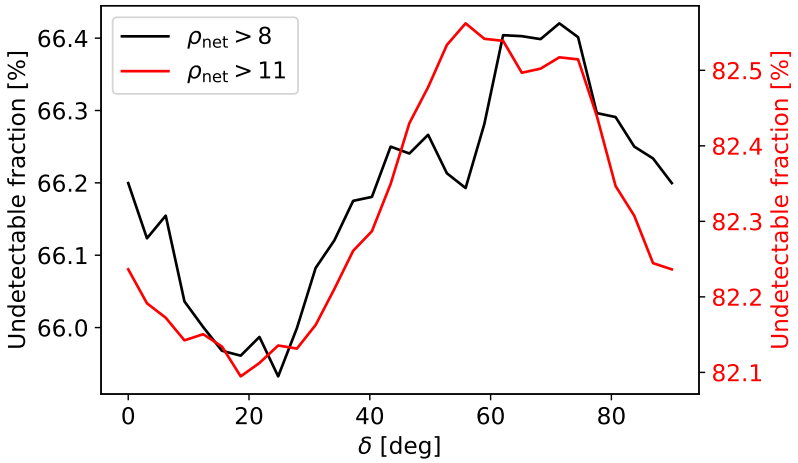

Figure 9: Fraction of BNS sources that have network SNR below 8 (left axis) or 11 (right axis) in a network of CE A and CE B as a function of their relative misalignment (see Table 1).

6 Conclusions

We conclude that in the limit where a CE B sees nearly all of the CBC sources (i.e., for BBHs) the most important thing that CE A can contribute is polarization coverage. In that case, a value of δ of $60^\circ - 70^\circ$ is desired. For sources for which selection effects are important, such as BNS, that same value will instead minimize the number of detections. However, for both type of sources, only a few percent of the sources can move from detectable to undetectable depending on the relative orientation angle. Given that tens to hundred of thousands of CBCs are expected per year, this small variation might not constitute a significant factor. One might investigate alternative figures of merit that might be more relevant for BNS specifically, e.g. sky localization [1] or performances for the loudest sources only.

7 Data availabilty

The Jupyter and Mathematica notebooks used to produce the data and plots in this document can be found in this GitHub repository.

8 Acknowledgements

SV acknowledges support from NSF award PHY-2207387. DB acknowledges support from NSF award PHY-2207264. BS acknowledges support from NSF award PHY-2207638.

References

[1] Bernard F. Schutz. Networks of gravitational wave detectors and three figures of merit. *Class. Quant. Grav.*, 28:125023, 2011.

[2] Antony C. Searle, Susan M. Scott, David E. McClelland, and L. Samuel Finn. Optimal location of a new interferometric gravitational wave observatory. *Phys. Rev. D*, 73:124014, Jun 2006.

[3] Nicolas Arnaud, Matteo Barsuglia, Marie-Anne Bizouard, Violette Brisson, Fabien Cavalier, Michel Davier, Patrice Hello, Stephane Kreckelbergh, and Edward K. Porter. Coincidence and coherent data analysis methods for gravitational wave bursts in a network of interferometric detectors. *Phys. Rev. D*, 68:102001, 2003.

[4] Salvatore Vitale. Three observational differences for binary black holes detections with second and third generation gravitational-wave detectors. *Phys. Rev. D*, 94(12):121501, 2016.